*Progress In Electromagnetics Research B, Vol. 60, 49–62, 2014*

# An Integral Equation Formulation for TM Scattering by a Conducting Cylinder Coated with an Inhomogeneous Dielectric/Magnetic Material

**Ahmed A. Sakr[1], Ezzeldin A. Soliman[2], and Alaa K. Abdelmageed[1, *]**

**Abstract**—A volume-surface integral equation (VSIE) formulation is developed for determining the electromagnetic TM scattering by a two-dimensional conducting cylinder coated with an inhomogeneous dielectric/magnetic material. The electric field integral equations (EFIEs) are utilized to derive the VSIE. The surface EFIE is applied to the conducting surface, while the volume EFIE is applied to the coating region. By employing the surface and equivalence principles, the problem is reduced into a set of coupled integral equations in terms of equivalent electric and magnetic currents radiating into unbounded space. The moment method is used to solve the integral equations. Numerical results for the bistatic radar cross section for different structures are presented. The well-known exact series-solution for a conducting circular cylinder coated with multilayers of homogeneous materials is used along with the available published data to validate the results. The influence of using coatings with double-positive (DPS) and/or double-negative (DNG) materials on the radar cross section is investigated.

## 1. INTRODUCTION

The topic of electromagnetic scattering has gained wide and growing consideration. This consideration is of practical importance in radars, antennas and measurements. Extensive research has been exerted in this field. One motivation behind the research is to meet the new emerging applications, and the other is to explore new methods for handling the scattering problems more efficiently. Extensive research has been conducted on the problem of coated conducting cylinders due to its importance in many applications. One of them is the protection of objects from the radar illumination where the coating can be used to acquire maximum radar scattering cross-section reduction. In antenna design, the coating can be used to reduce the aperture blockage caused by some mechanical structures which are placed in the vicinity of the antenna system.

The problem of electromagnetic scattering by a coated conducting two-dimensional cylinder has only an exact solution for a limited class of geometries provided that the coating material has homogeneous and isotropic properties. For these geometries (circular, elliptical), the scattered field can be expressed in terms of a set of eigenfunctions using the separation of variables method [1]. The problem of a dielectric coated conducting circular cylinder was first studied by Tang [2] where an exact series solution is developed by utilizing cylindrical eigenfunctions expansion. Richmond derived a series-solution for a coated conducting elliptic cylinder using Mathieu functions [3]. This approach has been exploited to study several other structures [4–7]. The method can be extended to handle a conducting cylinder with a multilayer coating [8–11].

When the coated cylinder has an arbitrary cross-section or when the coating material has inhomogeneous properties, the problem has to be attacked numerically. Several numerical techniques

*Received 15 March 2014, Accepted 17 May 2014, Scheduled 21 May 2014*

* Corresponding author: Alaa K. Abdelmageed (abdelmag@msn.com).

[1] Engineering Mathematics and Physics Department, Faculty of Engineering, Cairo University, Giza 12211, Egypt. [2] Department of Physics, School of Sciences and Engineering, The American University in Cairo, Egypt.

have been proposed to study this problem. In cases where the coating region is homogeneous or piecewise homogeneous, the surface integral equation (SIE) formulation is an efficient and suitable candidate [12]. Diversity of the SIE formulations have been adopted in the literature [13]. These formulations comprise the PMCHW formulation [14–16], the Müller formulation [17], and the single-source surface integral equation (SSIE) formulation [18–21]. The SIE formulations have been applied to investigate the problem of a dielectric coated conducting cylinder [22–26]. For the PMCHW and Müller formulations, the surfaces of the conductor and the dielectric are replaced by equivalent electric and magnetic surface current sources using the surface equivalence principle. These sources are radiating in unbounded space. By imposing the boundary conditions on the cylindrical surfaces, a set of coupled integral equations is obtained. These integral equations are formulated in terms of the unknown surface currents. To find these currents, the integral equations are solved using the method of moment (MoM) [27]. Once these currents are determined, the scattered fields and related parameters such as the radar cross section (RCS) are readily determined. For the SSIE formulation, only a single unknown source is utilized. This source could be an electric or magnetic surface current placed at the material boundaries. Thus, the PMCHW and Müller formulations utilize two unknown current sources at each material boundary, while the SSIE utilizes one unknown surface current source. Although the SSIE has an advantage of reducing the number of unknowns, it may result in increasing the computational complexity compared with the other two forms [21].

One disadvantage of the SIE is that it is only valid for coating materials having homogeneous properties. It can consider piecewise homogeneous coating materials [21]. Even for piecewise homogeneous materials, the efficiency of the SIE decreases as the number of the layers increases, since boundary conditions have to be imposed on the interfaces between coating layers. To overcome this deficiency, the surface-volume integral equation (SVIE) formulation has been applied to treat conducting objects coated with inhomogeneous materials [28–30]. In this approach, the surface and volume equivalence principles are employed where the original problem is replaced by a surface electric current at the conducting surface, and polarization currents in the volume of the coating. The unknown currents radiate into unbounded space. The surface integral equation is enforced at the conducting object, while the volume integral equation is applied to the volume of the coating. A set of coupled integral equations is obtained. These integrals are formulated in terms of the unknown surface and volume currents. To find these currents, the MoM is invoked. In the quest of reducing the number of unknowns and in resemblance with the SSIE, the VSIE has another variant for modeling the inhomogeneity. Instead of modeling the problem using the equivalent electric and magnetic current sources as unknown quantities, alternatively either the electric field or magnetic field can be used as a single unknown quantity [31–34]. This method will be denoted here as SVSIE.

A hybrid finite-element method has been applied to study conducting cylinders coated with inhomogeneous dielectric and/or magnetic materials [35]. In [36], the coupled finite boundary element method was used to combine the advantages of both the finite element method and the boundary element method. Other techniques such as the multifilament current model [37] and the on-surface radiation condition [38] have been proposed to treat the coated conducting cylinders. Several high frequency techniques have been devised for a dielectric coated conducting cylinders [39–44].

Most of the published works are concerned with either dielectric or magnetic coating materials. Works that address inhomogeneous dielectric/magnetic coating materials are limited [32, 35]. In [32] the SVSIE is utilized, and in [35] the hybrid finite element method is adopted. The results presented in these works are given for conducting cylinders coated with only one layer having homogeneous properties. The application of these methods to multilayer coatings has not been well-addressed. Hence, the efficiency of these works are not clearly manifested for handling dielectric/magnetic coatings having inhomogeneous properties. In this work, the VSIE is used to study the TM-scattering by a two-dimensional conducting cylinder coated with an inhomogeneous material. The profile of the relative permittivity and permeability is arbitrary. The coating may also be constructed of several layers. Each layer may have a nonunity relative permittivity and permeability. The interaction of electromagnetic waves with conducting objects coated with metamaterials has attracted recently the attention of many researchers [6, 45, 46]. This has tempted us to study the influence of using coating layers of metamaterials on the RCS. As outlined earlier, the surface equivalence principle is used to replace the conducting surface by a surface electric current. Also, the volume equivalence principle is used to replace the

coating region by polarization volume currents. Imposing the boundary conditions on the surface of the conducting cylinder, a surface EFIE is developed. Within the coating region, the volume EFIE is applied. The obtained integral equations are expressed in terms of the unknown equivalent currents. As the VSIE method is employed for modeling the scattering problem using the EFIEs, the developed formulation is given the acronym VSIE-EFIE. The unknown currents are obtained by solving the integral equations of this formulation using the MoM. The paper is organized as follows. In the next section, the formulation of the problem is presented. In Section 3, numerical results for the RCS for different structures are given. The impact of two types of coating materials on the results of the RCS are studied, namely the DPS and DNG materials. For the DPS materials, both the relative permittivity and relative permeability are positive, while for the DNG materials, both the relative permittivity and relative permeability are negative. Finally, some concluding remarks are given in Section 4.

## 2. FORMULATION

In this section, a set of coupled integral equations based on the VSIE-EFIE formulation is developed for the problem of electromagnetic scattering by a two-dimensional coated conducting cylinder. The TM wave scattering is considered. The geometry of the problem under consideration is depicted in Fig. 1. The figure shows a cross-sectional view of a coated perfectly electric conducting (PEC) cylinder along with the relevant coordinate system. The cylinder is assumed to be infinitely long in the $z$-direction. The conducting surface is bounded by contour $C$. The domain of the coating region is denoted by $\Omega$. The coating material is assumed to be linear and isotropic with permittivity $\varepsilon = \varepsilon_o\varepsilon_r(x,y)$ and permeability $\mu = \mu_o\mu_r(x,y)$ where $\varepsilon_o$ and $\mu_o$ are the free-space permittivity and permeability, respectively. The cylinder is embedded in free-space with a wavenumber $k_o = \omega\sqrt{\varepsilon_o\mu_o} = 2\pi/\lambda_o$, where $\lambda_o$ is the wavelength in free-space. The time dependence $e^{j\omega t}$ is assumed and suppressed throughout.

The cylinder is illuminated by an incident field $(\mathbf{E}^i, \mathbf{H}^i)$ which is polarized along the axis of the cylinder

$$\mathbf{E}^i = \mathbf{a}_z E_z^i(x,y) \tag{1}$$

$$\mathbf{H}^i = \mathbf{a}_x H_x^i(x,y) + \mathbf{a}_y H_y^i(x,y) \tag{2}$$

The total field $(\mathbf{E}, \mathbf{H})$ is the sum of the incident field and the scattered field $(\mathbf{E}^s, \mathbf{H}^s)$. Using the surface and volume equivalence principles [34], the conducting surface is replaced with a surface electric current $\mathbf{J}_c$, and the volume of the coating is replaced by volume polarization electric current $\mathbf{J}_p$ and magnetic current $\mathbf{M}_p$. These currents are radiating in unbounded free space. The scattered field $\mathbf{E}^s$ and the total field $\mathbf{E}$ are polarized in the $z$-direction as the incident field. Therefore,

$$E_z = E_z^i + E_z^s \tag{3}$$

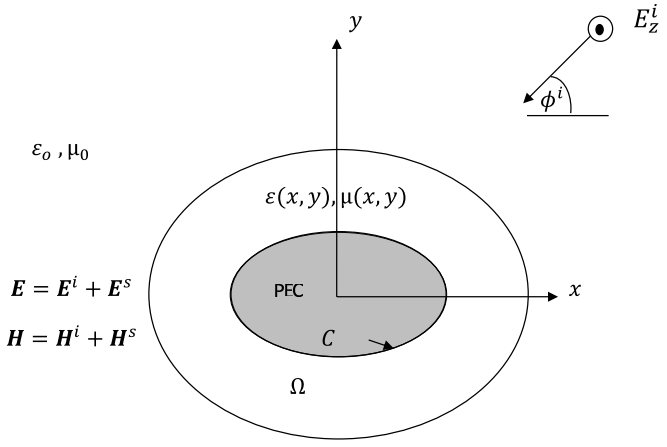


**Figure 1.** Cross-sectional view of a coated PEC cylinder illuminated by an incident wave.

On the contour $C$ of the conducting surface, the boundary conditions necessitate that the total tangential electric field should vanish. Hence,

$$E_z^i(x,y) = -E_z^s(x,y), \quad \text{on } C \tag{4}$$

The polarization currents are related to the total fields $(\mathbf{E}, \mathbf{H})$ through the relations [1]

$$\mathbf{J}_p(x,y) = \mathbf{a}_z\, j\omega\varepsilon_o[\varepsilon_r(x,y)-1]E_z(x,y), \quad \text{on } \Omega \tag{5}$$

$$\mathbf{M}_p(x,y) = M_{px}\mathbf{a}_x + M_{py}\mathbf{a}_y = j\omega\mu_o[\mu_r(x,y)-1]\mathbf{H}(x,y), \quad \text{on } \Omega \tag{6}$$

For a TM wave incidence, both $\mathbf{J}_c$ and $\mathbf{J}_p$ are along the $z$-direction, while $\mathbf{M}_p$ has two transverse components, namely $M_{px}$, $M_{py}$. In view of (3), Equation (5) can be equivalently written in the form

$$E_z^i(x,y) = \frac{J_p(x,y)}{j\omega\varepsilon_o(\varepsilon_r-1)} - E_z^s(x,y), \quad \text{on } \Omega \tag{7}$$

In (6), the polarization magnetic current is represented in terms of the total magnetic field, alternatively it can be expressed in terms of the total electric field as

$$\mathbf{M}_p = -\frac{\mu_r-1}{\mu_r}\nabla\times\mathbf{E} = -\frac{\mu_r-1}{\mu_r}\nabla\times\left(\mathbf{E}^i+\mathbf{E}^s\right) \tag{8}$$

or

$$\nabla\times\mathbf{E}^i = -\frac{\mu_r}{\mu_r-1}\mathbf{M}_p - \nabla\times\mathbf{E}^s, \quad \text{on } \Omega \tag{9}$$

Equation (9) can be split into the following two equations in the $x$- and $y$-directions

$$\frac{\partial E_z^i}{\partial y} = -\frac{\mu_r}{\mu_r-1}M_{px} - \frac{\partial E_z^s}{\partial y}, \quad \text{on } \Omega \tag{10}$$

$$-\frac{\partial E_z^i}{\partial x} = -\frac{\mu_r}{\mu_r-1}M_{py} + \frac{\partial E_z^s}{\partial x}, \quad \text{on } \Omega \tag{11}$$

The scattered field is induced due to $J_c$, $J_p$, $M_{px}$ and $M_{py}$. It can be expressed as [34]

$$E_z^s = -jk_o\eta A_z - \frac{\partial F_y}{\partial x} + \frac{\partial F_x}{\partial y} \tag{12}$$

where $\eta$ is the intrinsic impedance of free space. $\mathbf{A}$ and $\mathbf{F}$ are the magnetic and electric vector potentials, respectively. They are given as

$$\mathbf{A}(\boldsymbol{\rho}) = \int \mathbf{J}\left(\boldsymbol{\rho}'\right)\, G_o\left(\boldsymbol{\rho} \mid \boldsymbol{\rho}'\right)\, d\Gamma' \tag{13}$$

$$\mathbf{F}(\boldsymbol{\rho}) = \int \mathbf{M}\left(\boldsymbol{\rho}'\right)\, G_o\left(\boldsymbol{\rho} \mid \boldsymbol{\rho}'\right)\, d\Gamma' \tag{14}$$

where

$$G_o\left(\boldsymbol{\rho} \mid \boldsymbol{\rho}'\right) = -\frac{j}{4}H_o^2\left(k_o \mid \boldsymbol{\rho}-\boldsymbol{\rho}'\mid\right) \tag{15}$$

$\boldsymbol{\rho}$ and $\boldsymbol{\rho}'$ are the position vectors of the field and source points, respectively. $G_o$ is the two-dimensional Green's function, and $H_o^2$ is the zeroth-order Hankel function of the second kind. In (13) if $\mathbf{J}=\mathbf{J}_c$, the integration is performed on the contour $C$ of the conducting surface and $d\Gamma' = d\ell'$. On the other hand, if $\mathbf{J}=\mathbf{J}_p$ in (13) or $\mathbf{M}=\mathbf{M}_p$ in (14), the integration is performed on the coating region domain $\Omega$ and $d\Gamma' = dS'$. Substituting (13)–(15) in (12) produces

$$\begin{aligned} E_z^s(\mathrm{x},\mathrm{y}) = &-\frac{k_o\eta}{4}\int_C J_c\left(x',y'\right)\, H_0^2\left(k_oR\right)d\ell' - \frac{k_o\eta}{4}\iint_\Omega J_p\left(x',y'\right)H_0^2\left(k_oR\right)dx'dy' \\ &-\frac{j}{4}\frac{\partial}{\partial y}\iint_\Omega M_{px}\left(x',y'\right)H_0^2\left(k_oR\right)dx'dy' + \frac{j}{4}\frac{\partial}{\partial x}\iint_\Omega M_{py}\left(x',y'\right)H_0^2\left(k_oR\right)dx'dy' \end{aligned} \tag{16}$$

where

$$R = \sqrt{(x-x')^2 + (y-y')^2} \tag{17}$$

$(x, y)$ and $(x', y')$ are the coordinates of the field and source points, respectively. Equations (4), (7), (10) and (11) constitute the required relations needed to determine the four unknowns $J_c$, $J_p$, $M_{px}$ and $M_{py}$. On substituting for $E_z^s$, as given by (16), in these equations yields

$$\begin{aligned} E_z^i &= \frac{k_o\eta}{4}\int\limits_C J_c\, H_0^2\,(k_oR)\;\, d\ell' + \frac{k_o\eta}{4}\iint\limits_\Omega J_p\, H_o^2\,(k_oR\,)\;\, dx'dy' \\ &\quad + \frac{j}{4}\frac{\partial}{\partial y}\iint\limits_\Omega M_{px}\, H_o^2(k_oR)\; dx'dy' - \frac{j}{4}\frac{\partial}{\partial x}\iint\limits_\Omega M_{py}\, H_o^2\,(k_oR)\;\, dx'dy', \qquad \text{on } C \end{aligned} \tag{18}$$

$$\begin{aligned} E_z^i &= \frac{\eta J_p}{jk_o\,(\varepsilon_r - 1)} + \frac{k_o\eta}{4}\int\limits_C J_c\, H_o^2\,(k_oR)\;\, d\ell' + \frac{k_o\eta}{4}\iint\limits_\Omega J_p\, H_o^2\,(k_oR)\;\, dx'dy' \\ &\quad + \frac{j}{4}\frac{\partial}{\partial y}\iint\limits_\Omega M_{px}\, H_o^2\,(k_oR)\;\, dx'dy' - \frac{j}{4}\frac{\partial}{\partial x}\iint\limits_\Omega M_{py}\, H_o^2(k_oR)\; dx'dy', \qquad \text{on } \Omega \end{aligned} \tag{19}$$

$$\begin{aligned} \frac{\partial}{\partial y}E_z^i &= -\frac{\mu_r}{\mu_r - 1}M_{px} + \frac{k_o\eta}{4}\frac{\partial}{\partial y}\int\limits_C J_c\, H_o^2\,(k_oR)\;\, d\ell' + \frac{k_o\eta}{4}\frac{\partial}{\partial y}\iint\limits_\Omega J_p\, H_o^2\,(k_oR)\;\, dx'dy' \\ &\quad + \frac{j}{4}\frac{\partial^2}{\partial y^2}\iint\limits_\Omega M_{px}\, H_o^2(k_oR)\; dx'dy' - \frac{j}{4}\frac{\partial^2}{\partial y\partial x}\iint\limits_\Omega M_{py}\, H_o^2(k_oR)\; dx'dy', \qquad \text{on } \Omega \end{aligned} \tag{20}$$

$$\begin{aligned} \frac{\partial}{\partial x}E_z^i &= \frac{\mu_r}{\mu_r - 1}M_{py} + \frac{k_o\eta}{4}\frac{\partial}{\partial x}\int\limits_C J_c\, H_o^2\,(k_oR)\;\, d\ell' + \frac{k_o\eta}{4}\frac{\partial}{\partial x}\iint\limits_\Omega J_p\, H_o^2\,(k_oR)\;\, dx'dy' \\ &\quad + \frac{j}{4}\frac{\partial^2}{\partial y\partial x}\iint\limits_\Omega M_{px}\, H_o^2(k_oR)\; dx'dy' - \frac{j}{4}\frac{\partial^2}{\partial x^2}\iint\limits_\Omega M_{py}\, H_o^2\,(k_oR)\;\, dx'dy', \qquad \text{on } \Omega \end{aligned} \tag{21}$$

Equations (18)–(21) represent the VSIE-EFIE formulation for TM-scattering by a two-dimensional PEC cylinder coated with an inhomogeneous dielectric/magnetic material. All the integral equations are derived using the EFIEs. The first of these equations is a surface EFIE applied to the surface of the conductor, while the other three equations are volume EFIEs applied to the volume of the coating. In order to solve these equations, we follow the typical MoM procedure. The contour of the conducting surface is discretized into a set of $N_c$ line segments, while the coating region $\Omega$ is subdivided into $N_p$ nearly square cells. The surface current and volume polarization currents are approximated using subsectional pulse basis functions on their respective domains with amplitudes yet to be determined. On enforcing the resulting equations at the centers of these segments/cells using point matching, Equations (18)–(21) are converted into a set of $(N_c + 3N_p)$ linear equations. The matrix equation can be written as

$$\left[\begin{array}{c|ccc} A^{(1)} & A^{(2)} & A^{(3)} & A^{(4)} \\ \hline B^{(1)} & B^{(2)} & B^{(3)} & B^{(4)} \\ C^{(1)} & C^{(2)} & C^{(3)} & C^{(4)} \\ D^{(1)} & D^{(2)} & D^{(3)} & D^{(4)} \end{array}\right] \left[\begin{array}{c} \mathcal{J}_c \\ \hline \mathcal{J}_p \\ \mathcal{M}_x \\ \mathcal{M}_y \end{array}\right] = \left[\begin{array}{c} E^{(1)} \\ \hline E^{(2)} \\ E^{(3)} \\ E^{(4)} \end{array}\right] \tag{22}$$

where $A^{(1)}$ is a matrix of dimensions $N_c \times N_c$, $\{B^{(i)}, C^{(i)}, D^{(i)}$ for $i = 2:4\}$ are matrices of dimensions $N_p \times N_p$, $\{A^{(i)}$ for $i = 2:4\}$ are matrices of dimensions $N_c \times N_p$, and $\{B^{(1)}, C^{(1)}, D^{(1)}\}$ are matrices of dimensions $N_p \times N_c$. $E^{(1)}$, $E^{(2)}$ are vectors of the incident field evaluated at the centers of the line segments and cells, respectively. $E^{(3)}$, $E^{(4)}$ are vectors of $\frac{\partial E_z^i}{\partial y}$ and $\frac{\partial E_z^i}{\partial x}$, respectively, evaluated at the

centers of the cells. $E^{(1)}$ is a column vector of length $N_c$, while $E^{(2)}$, $E^{(3)}$, $E^{(4)}$ are column vectors of length $N_p$. Solving the matrix equation renders the vectors $\mathcal{J}_c$, $\mathcal{J}_p$, $\mathcal{M}_x$ and $\mathcal{M}_y$ which represent the amplitudes of the currents $J_c$, $J_p$, $M_{px}$ and $M_{py}$. To demonstrate the interaction of the conducting object and the coating material due to the excitation as monitored by the moment matrix, the matrix Equation (22) can be partitioned as illustrated by dashed lines into the following form

$$\begin{bmatrix} Z_{cc} & Z_{cd} \\ Z_{dc} & Z_{dd} \end{bmatrix} \begin{bmatrix} \mathcal{I}_c \\ \mathcal{I}_p \end{bmatrix} = \begin{bmatrix} \mathcal{E}_1 \\ \mathcal{E}_2 \end{bmatrix} \tag{23}$$

where the correspondence of the matrices and vectors in (23) with those in (22) is clear. $Z_{cc}$, $Z_{cd}$, $Z_{dc}$ and $Z_{dd}$ are submatrix blocks. $Z_{cc}$ is the moment matrix contribution of the conducting surface, and $Z_{dd}$ is the moment matrix contribution of the coating material. $Z_{cd}$ and $Z_{dc}$ represent the interaction between the conducting surface and the coating material.

The integrals involved in these equations can be evaluated using a suitable numerical quadrature procedure. However, when the integration is performed over a cell domain, we follow here the same approach adopted by Richmond [47]. In this approach, the integrals are evaluated analytically if the cell shapes are approximated by circles having the same area. The details will not be repeated here and may be found elsewhere [47, 48].

The solution of the matrix Equation (22) yields the unknown currents. Once these currents are obtained, the RCS can be easily computed. It is defined as

$$\mathrm{RCS}(\phi) = \lim_{\rho\to\infty} 2\pi\rho \left| \frac{E_z^s(\phi)}{E_z^i} \right|^2 \tag{24}$$

## 3. NUMERICAL RESULTS

To demonstrate the accuracy of the MoM-based VSIE-EFIE formulation, results are shown in Figs. 3–14. For Figs. 3–12, the incident field is a TM$_z$-polarized plane wave propagating in the $x$-direction. The results in Figs. 3–11 are presented for a circular PEC cylinder coated with multilayers of homogeneous materials. The structure of this multilayered coated cylinder is given in Fig. 2. The PEC cylinder may be coated with only one layer, two layers or generally $N$ layers. The radius of the PEC cylinder is $R_o$, and the outer radius of the $i$th-layer is $R_i$ where $i$ runs from 1 (the innermost layer) to $N$ (the outermost layer). Each layer is characterized by a permittivity $\varepsilon_i = \varepsilon_o\varepsilon_{ri}$, a permeability $\mu_i = \mu_o\mu_{ri}$ and wavenumber $k_i = k_o\sqrt{\mu_{ri}\varepsilon_{ri}}$, where $\varepsilon_{ri}$ and $\mu_{ri}$ are the relative permittivity and permeability, respectively. The exact series-solution for a circular PEC cylinder with a multilayer coating [11] is incorporated in the figures to solidify the accuracy of the results. Figs. 3–5 show the bistatic RCS for a one-layer coating. In Fig. 3, $R_o = \lambda_o$, $R_1 = 1.5\lambda_o$, $\varepsilon_r = 2$, $\mu_r = 2$. The results show complete

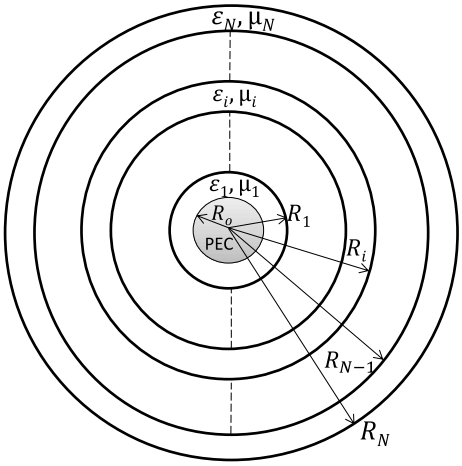


**Figure 2.** Structure of a PEC circular cylinder coated with multilayers of homogeneous materials.

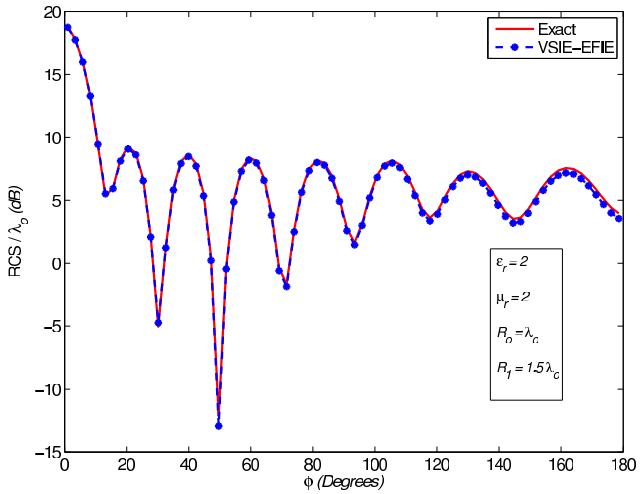


**Figure 3.** Bistatic RCS for a circular PEC cylinder with a one-layer coating, $R_o = \lambda_o$, $R_1 = 1.5\lambda_o$, $\varepsilon_r = 2$, $\mu_r = 2$.

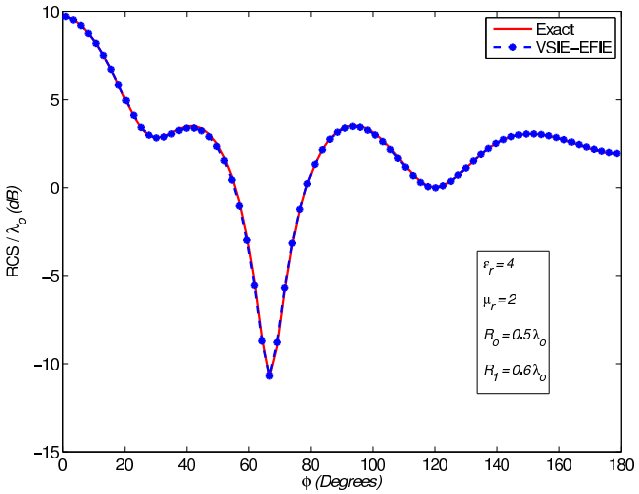


**Figure 4.** Bistatic RCS for a circular PEC cylinder with a one-layer DPS coating, $R_o = 0.5\lambda_o$, $R_1 = 0.6\lambda_o$, $\varepsilon_r = 4$, $\mu_r = 2$.

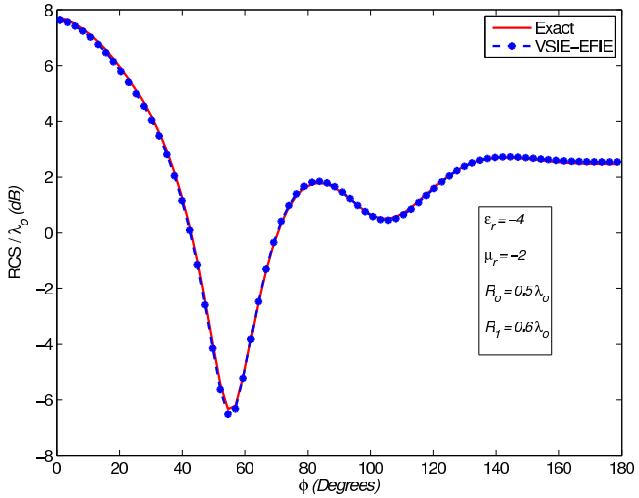


**Figure 5.** Bistatic RCS for a circular PEC cylinder with a one-layer DNG coating, $R_o = 0.5\lambda_o$, $R_1 = 0.6\lambda_o$, $\varepsilon_r = -4$, $\mu_r = -2$.

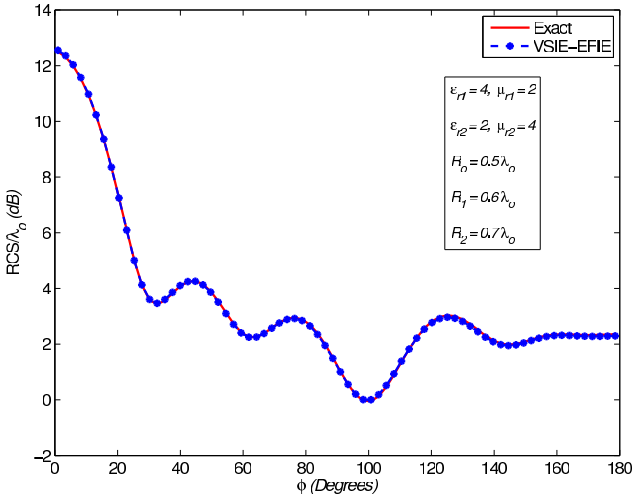


**Figure 6.** Bistatic RCS for a circular PEC cylinder with a two-layer coating, $R_o = 0.5\lambda_o$, $R_1 = 0.6\lambda_o$, $R_2 = 0.7\lambda_o$, $\varepsilon_{r1} = 4$, $\mu_{r1} = 2$, $\varepsilon_{r2} = 2$, $\mu_{r2} = 4$.

agreement with the series solution. To study the impact of DPS and DNG materials, results are presented in Figs. 4 and 5 for a one-layer coating having either a DPS or DNG material. For both figures, $R_o = 0.5\lambda_o$, $R_1 = 0.6\lambda_o$. In Fig. 4, $\varepsilon_r = 4$, $\mu_r = 2$, and in Fig. 5, $\varepsilon_r = -4$, $\mu_r = -2$. The results show a complete agreement with the exact solution. Observing these results, one can note that the DNG coating has a lower backscattering and a higher forward scattering. To inspect this point deeply, the values of both the backscattering $B_{sc}$ and forward scattering $F_{sc}$ for different structures are listed in Table 1. Examining the table, it is obvious that the values of $B_{sc}$ or $F_{sc}$ are fluctuating as the coating thickness increases for certain $|\varepsilon_r|$ and $|\mu_r|$. Therefore, the coating type (DNG or DPS) which has a lower value of $B_{sc}$ or $F_{sc}$ for certain $|\varepsilon_r|$ and $|\mu_r|$ depends on the thickness of the coating material.

Results for a two-layer coating are shown in Figs. 6–10. In Figs. 6 and 7, conventional (DPS) materials are used for both layers. In Fig. 6, $R_o = 0.5\lambda_o$, $R_1 = 0.6\lambda_o$, $R_2 = 0.7\lambda_o$, $\varepsilon_{r_1} = 4$, $\mu_{r1} = 2$, $\varepsilon_{r_2} = 2$, $\mu_{r2} = 4$, while in Fig. 7, $R_o = 0.7\lambda_o$, $R_1 = 0.8\lambda_o$, $R_2 = 0.9\lambda_o$, $\varepsilon_{r_1} = 6$, $\mu_{r1} = 3$, $\varepsilon_{r_2} =$

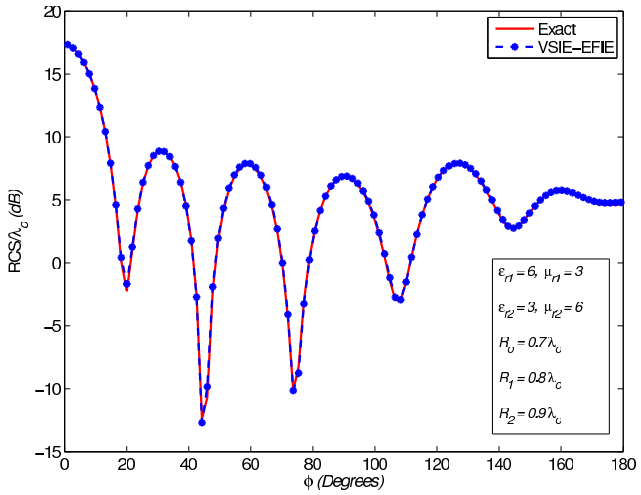


**Figure 7.** Bistatic RCS for a circular PEC cylinder with a two-layer coating, $R_o = 0.7\lambda_o$, $R_1 = 0.8\lambda_o$, $R_2 = 0.9\lambda_o$, $\varepsilon_{r1} = 6$, $\mu_{r1} = 3$, $\varepsilon_{r2} = 3$, $\mu_{r2} = 6$.

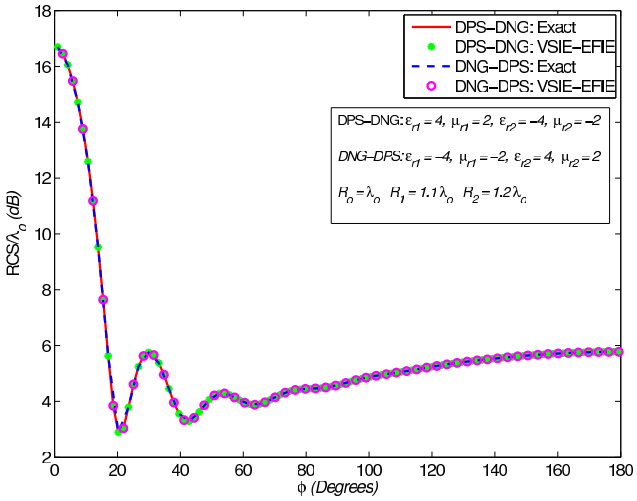


**Figure 8.** Bistatic RCS for a circular PEC cylinder with a two-layer coating, $R_o = \lambda_o$, $R_1 = 1.1\lambda_o$, $R_2 = 1.2\lambda_o$. DPS-DNG coating: $\varepsilon_{r1} = 4$, $\mu_{r1} = 2$, $\varepsilon_{r2} = -4$, $\mu_{r1} = -2$. DNG-DPS coating: $\varepsilon_{r1} = -4$, $\mu_{r1} = -2$, $\varepsilon_{r2} = 4$, $\mu_{r1} = 2$.

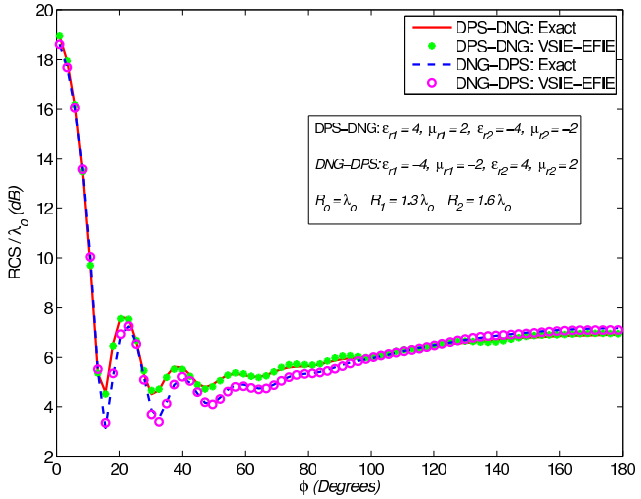


**Figure 9.** Bistatic RCS for a circular PEC cylinder with a two-layer coating, $R_o = \lambda_o$, $R_1 = 1.3\lambda_o$, $R_2 = 1.6\lambda_o$. DPS-DNG coating: $\varepsilon_{r1} = 4$, $\mu_{r1} = 2$, $\varepsilon_{r2} = -4$, $\mu_{r2} = -2$. DNG-DPS coating: $\varepsilon_{r1} = -4$, $\mu_{r1} = -2$, $\varepsilon_{r2} = 4$, $\mu_{r2} = 2$.

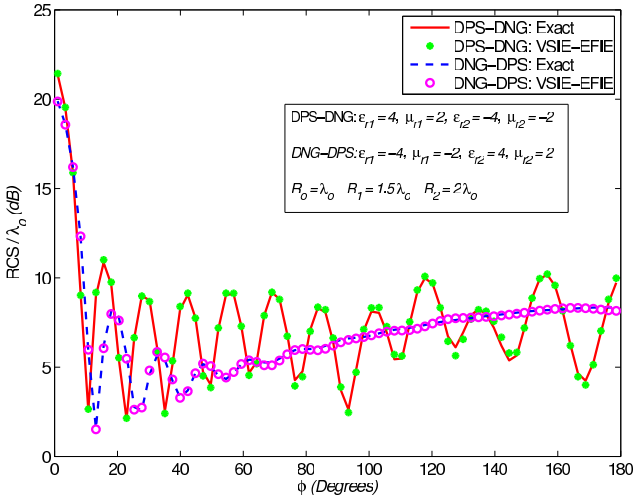


**Figure 10.** Bistatic RCS for a circular PEC cylinder with a two-layer coating, $R_o = \lambda_o$, $R_1 = 1.5\lambda_o$, $R_2 = 2.0\lambda_o$. DPS-DNG coating: $\varepsilon_{r1} = 4$, $\mu_{r1} = 2$, $\varepsilon_{r2} = -4$, $\mu_{r2} = -2$. DNG-DPS coating: $\varepsilon_{r1} = -4$, $\mu_{r1} = -2$, $\varepsilon_{r2} = 4$, $\mu_{r2} = 2$.

3, $\mu_{r2} = 6$. A comparison of the VSIE-EFIE results to the exact series solution shows a complete agreement. Fig. 8 shows the results of both DNG-DPS and DPS-DNG coatings. Both structures have $R_o = 1.0\lambda_o$, $R_1 = 1.1\lambda_o$, $R_2 = 1.2\lambda_o$. For DPS-DNG coating, $\varepsilon_{r_1} = 4$, $\mu_{r1} = 2$, $\varepsilon_{r_2} = -4$, $\mu_{r2} = -2$, while for DNG-DPS coating, $\varepsilon_{r_1} = -4$, $\mu_{r1} = -2$, $\varepsilon_{r_2} = 4$, $\mu_{r2} = 2$. As is evident, the results of the DNG-DPS and the DPS-DNG structures have an excellent agreement with the exact series solution. It is also observed that both the DNG-DPS and DPS-DNG structures have exactly the same RCS pattern. We examined this point extensively for different two-layer coatings assuming that the thickness of the layers is the same and both the DNG and DPS layers have the same $|\varepsilon_r|$ and $|\mu_r|$. For the cases studied,

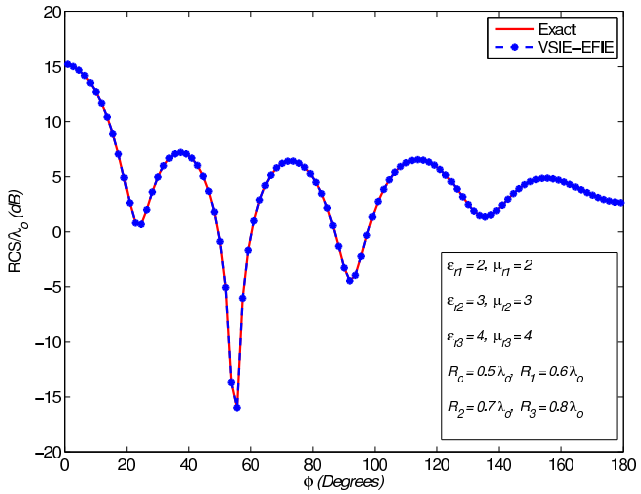


**Figure 11.** Bistatic RCS for a circular PEC cylinder with a three-layer coating, $R_o = 0.5\lambda_o$, $R_1 = 0.6\lambda_o$, $R_2 = 0.7\lambda_o$, $R_3 = 0.8\lambda_o$, $\varepsilon_{r1} = 2$, $\mu_{r1} = 2$, $\varepsilon_{r2} = 3$, $\mu_{r2} = 3$, $\varepsilon_{r3} = 4$, $\mu_{r3} = 4$.

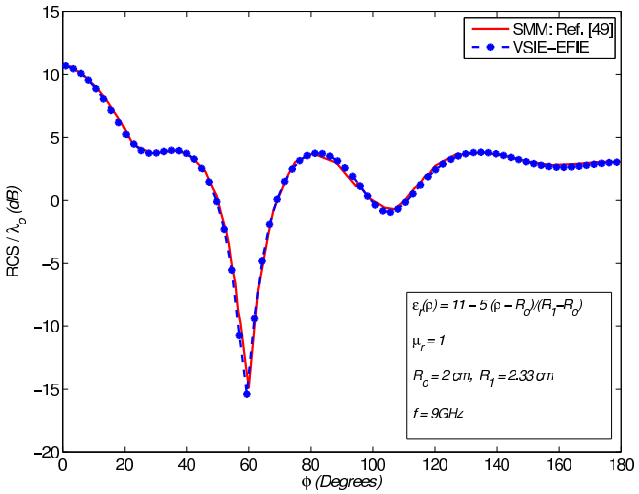


**Figure 12.** Bistatic RCS of a circular PEC cylinder coated with an inhomogeneous dielectric. $f = 9\,\text{GHz}$, $R_o = 2.0\,\text{cm}$, $R_1 = 2.33\,\text{cm}$, $\varepsilon_r(\rho) = 11 - 5(\rho - R_o)/(R_1 - R_o)$, $\mu_r = 1$.

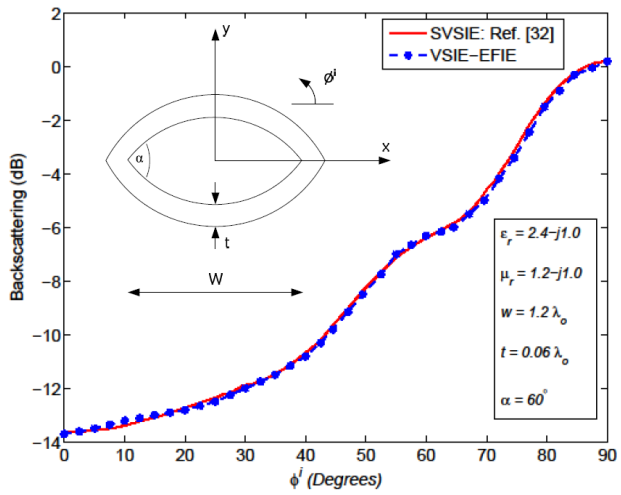


**Figure 13.** Backscattering RCS of an ogival PEC cylinder coated with one layer. $\varepsilon_r = 2.4 - j1.0$, $\mu_r = 1.2 - j1.0$.

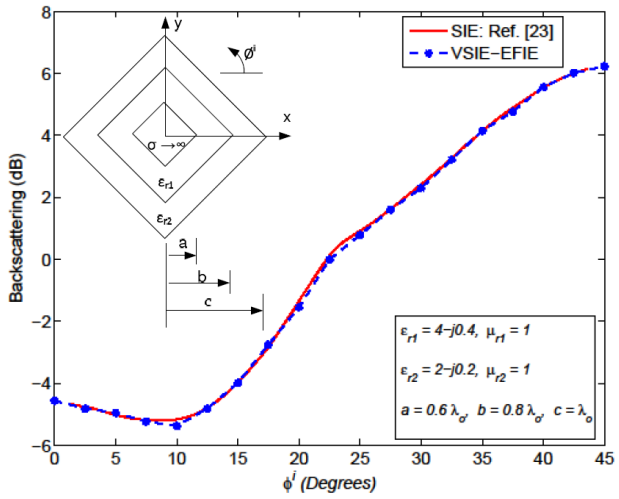


**Figure 14.** Backscattering RCS of a square PEC cylinder coated with two dielectric layers. $\varepsilon_{r1} = 4.0 - j0.4$, $\varepsilon_{r2} = 2.0 - j0.2$, $\mu_{r1} = \mu_{r2} = 1$.

we have found that the DNG-DPS and the DPS-DNG coatings have the same RCS for thin coating layers in the order of $0.1\lambda_o$. When the thickness of the layers begins to increase, a deviation starts. Figs. 9 and 10 show the RCS for a layer thickness equal to $0.3\lambda_o$ and $0.5\lambda_o$, respectively. In Fig. 9, $R_o = 1.0\lambda_o$, $R_1 = 1.3\lambda_o$, $R_2 = 1.6\lambda_o$, while in Fig. 10, $R_o = 1.0\lambda_o$, $R_1 = 1.5\lambda_o$, $R_2 = 2.0\lambda_o$. For both figures, the DPS layer has $\varepsilon_r = 4$, $\mu_r = 2$ and the DNG layer has $\varepsilon_r = -4$, $\mu_r = -2$. The figures show a complete agreement between the VSIE-EFIE and the exact solution. Fig. 9 reveals a discrepancy between the two patterns for a layer thickness equal to $0.3\lambda_o$ although they still have a similar behavior near the backscattering direction. This discrepancy becomes clearly conspicuous in Fig. 10 for layer thickness equal to $0.5\lambda_o$. It also seems that the DNG-DPS coating in this example has the effect of damping the oscillations of the RCS pattern in the forward scattering direction while the DPS-DNG experiences this oscillatory behavior.

**Table 1.** Backscattering $B_{sc}$ (dB) and forward-scattering $F_{sc}$ (dB) for one-layer coated PEC circular cylinder.

| $R_o$ | $R_1$ | $\lvert\varepsilon_r\rvert$ | $\lvert\mu_r\rvert$ | DPS | | DNG | |
|---|---|---|---|---|---|---|---|
| | | | | $B_{sc}$ | $F_{sc}$ | $B_{sc}$ | $F_{sc}$ |
| $0.5\lambda_o$ | $0.6\lambda_o$ | 4 | 2 | 9.71 | 1.94 | 7.64 | 2.54 |
| $0.5\lambda_o$ | $0.8\lambda_o$ | 4 | 2 | 12.16 | 4.65 | 12.17 | 2.74 |
| $0.5\lambda_o$ | $1.0\lambda_o$ | 4 | 2 | 12.36 | 3.17 | 15.47 | 3.83 |
| $0.5\lambda_o$ | $0.6\lambda_o$ | 2 | 4 | 8.69 | 1.96 | 7.61 | 2.39 |
| $0.5\lambda_o$ | $0.8\lambda_o$ | 2 | 4 | 11.00 | 3.59 | 11.17 | 4.54 |
| $0.5\lambda_o$ | $1.0\lambda_o$ | 2 | 4 | 11.69 | 3.83 | 14.92 | 9.37 |
| $0.7\lambda_o$ | $0.8\lambda_o$ | 4 | 2 | 12.07 | 3.08 | 10.43 | 3.79 |
| $0.7\lambda_o$ | $1.0\lambda_o$ | 4 | 2 | 14.60 | 5.17 | 13.25 | 5.12 |
| $0.7\lambda_o$ | $1.2\lambda_o$ | 4 | 2 | 15.39 | 5.87 | 17.17 | 6.73 |
| $0.7\lambda_o$ | $0.8\lambda_o$ | 6 | 3 | 14.42 | 4.26 | 12.89 | 3.82 |
| $0.7\lambda_o$ | $1.0\lambda_o$ | 6 | 3 | 11.71 | 4.41 | 16.68 | 5.43 |
| $0.7\lambda_o$ | $1.2\lambda_o$ | 6 | 3 | 16.65 | 4.95 | 16.42 | 6.67 |
| $0.7\lambda_o$ | $0.8\lambda_o$ | 2 | 2 | 10.54 | 3.42 | 15.95 | 6.34 |
| $0.7\lambda_o$ | $1.0\lambda_o$ | 2 | 2 | 15.98 | 5.14 | 14.83 | 6.64 |
| $0.7\lambda_o$ | $1.2\lambda_o$ | 2 | 2 | 15.92 | 4.85 | 17.03 | 10.54 |

Shown in Fig. 11 are the results of a three-layer coating with $R_o = 0.5\lambda_o$, $R_1 = 0.6\lambda_o$, $R_2 = 0.7\lambda_o$, $R_3 = 0.8\lambda_o$, $\varepsilon_{r_1} = 2$, $\mu_{r1} = 2$, $\varepsilon_{r_2} = 3$, $\mu_{r2} = 3$, $\varepsilon_{r_3} = 4$, $\mu_{r3} = 4$. The results have a good agreement with the series solution.

To assert further the validity of our method, we applied it to three different structures as shown in Figs. 12–14. Fig. 12 shows the bistatic RCS of a PEC cylinder coated with inhomogeneous dielectric whose permittivity is given as: $\varepsilon_r(\rho) = 11 - 5(\rho - R_o)/(R_1 - R_o)$ with $R_o \leq \rho \leq R_1$, $R_o = 2.0\,\text{cm}$, $R_1 = 2.33\,\text{cm}$, and frequency $f = 9\,\text{GHz}$. The results demonstrate a good agreement with those obtained from [49] using the scattering matrix method (SMM). The last two figures concern the application of the VSIE-EFIE to coated cylinders of arbitrary cross-section. The coating materials are lossy. Fig. 13 shows the backscattering RCS from ogival PEC cylinder coated with one layer of $\epsilon_r = 2.4 - j1.0$, $\mu_r = 1.2 - j1.0$. The results obtained using the SVSIE [32] are incorporated for comparison where a good agreement is realized. Fig. 14 shows the backscattering RCS from square PEC cylinder coated with double layers of lossy dielectrics of $\varepsilon_{r1} = 4 - j0.4$, $\varepsilon_{r2} = 2 - j0.2$ and $\mu_{r1} = \mu_{r2} = 1$. The results obtained using the SIE [23] are incorporated for comparison where a good agreement is achieved.

## 4. CONCLUSION

A VSIE-EFIE formulation is presented for studying the electromagnetic scattering by a two-dimensional PEC cylinder coated with an inhomogeneous dielectric/magnetic material. The case of a TM incident wave is considered. With using the surface and volume equivalence principles, the problem has been formulated in terms of equivalent surface and volume polarization currents. A set of coupled integral equation is derived in terms of these currents. The MoM has been used to solve these integral equations. A comparison with the eigenfunction solution for a circular PEC cylinder with a multilayer homogeneous coating has proved to have an excellent agreement. The method has also been applied to cylinders of arbitrary cross-section with lossy coating materials. The results are compared to the available published data where a good agreement is achieved. The impact of using DPS and DNG coating materials for a circular cylinder on the computed RCS has been investigated. Using one-layer coating of either DNG or DPS, we have found that the values of $B_{sc}$ and $F_{sc}$ are fluctuating with the increase of coating thickness. So, specifying which of the coating types (DNG or DPS) has a lower value of $B_{sc}$ or $F_{sc}$ for certain

$|\varepsilon_r|$ and $|\mu_r|$ depends on the thickness of the coating material. For two-layer coatings, we have found that the DPS-DNG and DNG-DPS coatings have very similar RCS patterns for equal and thin layers in the order of $0.1\lambda_o$. As the layer thickness begins to increase, a deviation occurs and the two patterns become distinct for thick layers. However, we have noticed that the two patterns have a nearly similar behavior in the neighborhood of the backscattering direction up to a layer thickness equal to $0.3\lambda_o$.

## APPENDIX A. SCATTERING BY PEC CIRCULAR CYLINDER COATED WITH MULTILAYERS OF HOMOGENEOUS MATERIALS

The closed series-solution for electromagnetic scattering by a circular PEC cylinder coated with multilayers of homogeneous materials is given in this appendix. The details of the derivation can be found in [11]. The structure of this cylinder is depicted in Fig. 2. It is illuminated by a $TM$-polarized incident wave propagating in the $x$-direction $\mathbf{E}^i = \mathbf{a}_z\, E_o e^{-jk_o x}$. The incident field can be expanded in terms of cylindrical functions as follows

$$\mathbf{E}^i = \mathbf{a}_z\, E_o \sum_{n=-\infty}^{\infty} j^{-n} J_n(k_o\rho) e^{jn\phi} \tag{A1}$$

where $J_n$ is the Bessel function of order $n$. The scattered field can be expressed as

$$E_z^s = E_o \sum_{n=-\infty}^{\infty} a_n H_n^2(k_o\rho) e^{jn\phi} \tag{A2}$$

while the total field in the $i$th-layer is given by

$$E_z^{(i)} = E_o \sum_{n=-\infty}^{\infty} \left[ C_n^{(i)} H_n^1(k_i\rho) + D_n^{(i)} H_n^1(k_i\rho) \right] e^{jn\phi} \tag{A3}$$

where $H_n^1$ and $H_n^2$ are the $n$th-order Hankel functions of the first and second kind, respectively. $a_n$, $C_n^{(i)}$ and $D_n^{(i)}$ are unknown quantities to be determined. Applying the boundary conditions at $\rho = R_i$ for $1 \le i \le N$ yields

$$a_n = -j^{-n} \frac{J_n(k_o R_N) - R_E^{(N)} J_n'(k_o R_N)}{H_n^2(k_o R_N) - R_E^{(N)} H_n^{2'}(k_o R_N)} \tag{A4}$$

$$R_E^{(i)} = \sqrt{\frac{\varepsilon_{i+1}\mu_i}{\mu_{i+1}\varepsilon_i}} \frac{H_n^1(k_i R_i) + \dfrac{D_n^{(i)}}{C_n^{(i)}} H_n^2(k_i R_i)}{H_n^{1'}(k_i R_i) + \dfrac{D_n^{(i)}}{C_n^{(i)}} H_n^{2'}(k_i R_i)}, \qquad 1 \le i \le N \tag{A5}$$

$$\frac{D_n^{(i+1)}}{C_n^{(i+1)}} = -\frac{H_n^1(k_{i+1} R_i) - R_E^{(i)} H_n^{1'}(k_{i+1} R_i)}{H_n^2(k_{i+1} R_i) - R_E^{(i)} H_n^{2'}(k_{i+1} R_i)}, \qquad 1 \le i \le N-1 \tag{A6}$$

Since the tangential electric field vanishes at the conducting surface $\rho = R_o$, we obtain

$$\frac{D_n^{(1)}}{C_n^{(1)}} = -\frac{H_n^1(k_1 R_o)}{H_n^2(k_1 R_o)} \tag{A7}$$

Starting with (A7), $R_E^{(N)}$ can be computed using a recursive procedure to calculate $R_E^{(i)}$ for $i = 1$ to $i = N$, and $\frac{D_n^{(i+1)}}{C_n^{(i+1)}}$ for $i = 1$ to $i = N-1$. Once $R_E^{(N)}$ is computed, $a_n$ in (A4) and hence the scattered field in (A2) can be calculated.

## REFERENCES


1. Balanis, C. A., *Advanced Engineering Electromagnetics*, John Wiley, New York, 1989.
2. Tang, C. C. H., "Backscattering from dielectric-coated infinite cylindrical obstacles," *J. Appl. Phys.*, Vol. 28, 628–633, 1957.
3. Richmond, J. H., "Scattering by a conducting elliptic cylinder with dielectric coating," *Radio Sci.*, Vol. 23, 1061–1066, 1988.
4. Kakogiannos, N. B. and J. A. Roumeliotis, "Electromagnetic scattering from an infinite elliptic metallic cylinder coated by a circular dielectric one," *IEEE Trans. Microwave Theory Tech.*, Vol. 38, 1660–1666, 1990.
5. Roumeliotis, J. A., H. K. Manthopoulos, and V. K. Manthopoulos, "Electromagnetic scattering from an infinite circular metallic cylinder coated by an elliptic dielectric one," *IEEE Trans. Microwave Theory Tech.*, Vol. 41, 862–869, 1993.
6. Li, C. and Z. Shen, "Electromagnetic scattering by a conducting cylinder coated with metamaterials," *Progress In Electromagnetics Research*, Vol. 42, 91–105, 2003.
7. Zouros, G. P., D. P. Kanoussis, and J. A. Roumeliotis, "Scattering by an infinite circular metallic cylinder coated by a lossless or lossy elliptical cylinder: Closed-form solutions," *7th European Conference on Antennas and Propagation (EuCAP)*, 2343–2347, Gothenburg, Sweden, 2013.
8. Bussy, H. E. and J. H. Richmond, "Scattering by a lossy dielectric circular cylindrical multilayer numerical values," *IEEE Trans. Antennas Propagat.*, Vol. 23, 723–725, 1975.
9. Sebak, A., L. Shafai, and H. A. Ragheb, "Electromagnetic wave scattering by a two-layered piecewise homogeneous confocal elliptic cylinder," *Radio Sci.*, Vol. 26, 111–119, 1991.
10. Caorsi, S., M. Pastorino, and M. Raffetto, "Scattering by a conducting elliptic cylinder with a multilayer dielectric coating," *Radio Sci.*, Vol. 32, 2155–2166, 1997.
11. Lin, J. M., *Theory and Computation of Electromagnetic Fields*, J. Wiley IEEE Press, Hobkon, New Jersey, 2010.
12. Poggio, A. J. and E. K. Miller, "Integral equation solutions of three-dimensional scattering problems," *Computer Techniques for Electromagnetics*, R. Mittra (ed.), Ch. 4, 129–163, Pergamon Press, New York, 1973.
13. Sheng, X. Q., J. M. Jin, J. Song, W. C. Chew, and C. C. Lu, "Solution of combined field integral equation using multilevel fast multipole algorithm for scattering by homogeneous bodies," *IEEE Trans. Antennas Propagat.*, Vol. 46, 1718–1726, 1998.
14. Wu, T. K. and L. L. Tsai, "Scattering from arbitrarily-shaped lossy dielectric bodies of revolution," *Radio Sci.*, Vol. 12, 709–718, 1977.
15. Umashankar, K., A. Taflove, and S. M. Rao, "Electromagnetic scattering by arbitrary shaped three-dimensional homogeneous lossy dielectric objects," *IEEE Trans. Antennas Propagat.*, Vol. 34, 758–766, 1986.
16. Harrington, R. F., "Boundary integral formulations for homogeneous material bodies," *Journal of Electromagnetic Waves and Applications*, Vol. 3, No. 1, 1–15, 1989.
17. Müller, C., *Foundation of the Mathematical Theory of Electromagnetic Waves*, Springer-Verlag, Berlin, 1969.
18. Glisson, A. W., "An integral equation for electromagnetic scattering from homogeneous dielectric bodies," *IEEE Trans. Antennas Propagat.*, Vol. 32, 173–175, 1984.
19. Swatek, D. R. and I. R. Ciric, "Single source integral equation for wave scattering by multiply-connected dielectric cylinders," *IEEE Trans. Magnetics*, Vol. 32, 878–881, 1996.
20. Swatek, D. R. and I. R. Ciric, "A recursive single-source surface integral equation analysis for wave scattering by heterogeneous dielectric bodies," *IEEE Trans. Antennas Propagat.*, Vol. 48, 1175–1185, 2000.
21. Menshov, A. and V. Okhmatovski, "New single-source surface integral equations for scattering on penetrable cylinders and current flow modeling in 2-D conductors," *IEEE Trans. Microwave Theory Tech.*, Vol. 61, 341–350, 2013.

22. Huddleston, P. L., L. N. Medgyesi-Mitschang, and J. M. Putnam, "Combined field integral equation formulation for scattering by dielectrically coated conducting bodies," *IEEE Trans. Antennas Propagat.*, Vol. 34, 510–520, 1986.
23. Arvas, E., M. Ross, and Y. Qian, "TM scattering from a conducting cylinder of arbitrary cross-section covered by multiple layers of lossy dielectrics," *IEE Proc.*, Pt. H, Vol. 135, 226–230, 1988.
24. Arvas, E. and T. K. Sarkar, "RCS of two-dimensional structures consisting of both dielectrics and conductors of arbitrary crosssection," *IEEE Trans. Antennas Propagat.*, Vol. 37, 546–554, 1989.
25. Rao, S. M., C. C. Cha, R. L. Cravey, and D. L. Wilkes, "Electromagnetic scattering from arbitrary shaped conducting bodies coated with lossy materials of arbitrary thickness," *IEEE Trans. Antennas Propagat.*, Vol. 39, 627–631, 1991.
26. Swatek, D. R. and I. R. Ciric, "Single integral equation for wave scattering by a layered dielectric cylinder," *IEEE Trans. Magnetics*, Vol. 34, 2724–2727, 1998.
27. Harrington, R. F., *Field Computation by Moment Methods*, Macmillan, New York, 1968, Reprinted by Krieger Publishing Co., Melbourne, FL, 1982.
28. Min, X., W. Sun, W. J. Gesang, and K. M. Chen, "An efficient formulation to determine the scattering characteristics of a conducting body with thin magnetic coatings," *IEEE Trans. Antennas Propagat.*, Vol. 39, 448–454, 1991.
29. Lin, C. S. and M. T. Yaqoob, "Scattering from a conducting surface coated with multilayers of lossy dielectric material (transverse electric polarization)," *J. Appl. Phys.*, Vol. 72, 3005–3008, 1992.
30. Lin, C. S. and M. T. Yaqoob, "An efficient formulation to find the scattering field of a conducting cylinder coated with lossy magnetic material," *J. Appl. Phys.*, Vol. 73, 4038–4041, 1993.
31. Jin, J. M., V. V. Liepa, and C. T. Tai, "A volume-surface integral equation for electromagnetic scattering by inhomogeneous cylinders," *Journal of Electromagnetic Waves and Applications*, Vol. 2, Nos. 5–6, 573–588, 1988.
32. Jin, J. M., and V. V. Liepa, "Simple moment method program for computing scattering from complex cylindrical obstacles," *IEE Proc.*, Pt. H, Vol. 136, 321–329, 1989.
33. Volakis, J. L., "Alternative field representations and integral equations for modeling inhomogeneous dielectrics," *IEEE Trans. Microwave Theory Tech.*, Vol. 40, 604–608, 1992.
34. Volakis, J. L. and K. Sertel, *Integral Equation Methods for Electromagnetics*, Scitech Publishing, Raleigh, NC, 2012.
35. Jin, J. M. and V. V. Liepa, "Application of hybrid finite element method to electromagnetic scattering from coated cylinders," *IEEE Trans. Antennas Propagat.*, Vol. 36, 50–54, 1988.
36. Wu, K. L., G. Y. Delisle, and D. G. Fang, "EM scattering of an arbitrary multiple dielectric coated conducting cylinder by coupled finite boundary element method," *IEE Proc.*, Pt. H, Vol. 137, 1–4, 1990.
37. Leviatan, Y., A. Boag, and A. Boag, "Analysis of electromagnetic scattering from dielectrically coated conducting cylinders using a multifilament current model," *IEEE Trans. Antennas Propagat.*, Vol. 36, 1602–1607, 1988.
38. Chen, Z. N. and W. X. Zhang, "Electromagnetic scattering from a dielectric coated cylinder using OSRC-GMT," *Electron. Lett.*, Vol. 29, 853–854, 1993.
39. Rao, T. C. K. and M. A. K. Hamid, "G.T.D. analysis of scattering from a dielectric-coated conducting cylinder," *IEE Proc.*, Pt. H, Vol. 127, 143–153, 1980.
40. Wang, N., "Electromagnetic scattering from a dielectric coated cylinder," *IEEE Trans. Antennas Propagat.*, Vol. 33, 960–963, 1985.
41. Kim, H. T. and N. Wang, "UTD solution for electromagnetic scattering by a circular cylinder with thin lossy coatings," *IEEE Trans. Antennas Propagat.*, Vol. 37, 1463–1472, 1989.
42. Tanyer, S. G. and R. G. Olsen, "High-frequency scattering by a conducting circular cylinder coated with a lossy dielectric of nonuniform thickness," *IEEE Trans. Antennas Propagat.*, Vol. 45, 689–697, 1997.
43. Hussar, P., "A uniform GTD treatment of surface diffraction by impedance and coated cylinders," *IEEE Trans. Antennas Propagat.*, Vol. 46, 998–1008, 1998.

44. Goto, K., L. H. Loc, T. Kawana, and T. Ishihara, "Extended UTD solution for scattered fields by a coated conducting cylinder," *Antennas and Propagation Society International Symposium (APSURSI)*, 1–2, Chicago, IL, 2012.
45. Sun, J., W. Sun, T. Jiang, and Y. Feng, "Directive electromagnetic radiation of a line source scattered by a conducting cylinder coated with left-handed metamaterial," *Microwave & Opt. Technol. Lett.*, Vol. 47, 274–279, 2005.
46. Zainud-Deen, S. H., A. Z. Botros, and M. S. Ibrahim, "Scattering from bodies coated with metamaterial using FDFD method," *Progress In Electromagnetics Research B*, Vol. 2, 279–290, 2008.
47. Richmond, J. H., "Scattering by a dielectric cylinder of arbitrary cross-section shape," *IEEE Trans. Antennas Propagat.*, Vol. 13, 334–341, 1965.
48. Peterson, A. F., S. L. Ray, and R. Mittra, *Computational Methods for Electromagnetics*, IEEE Press, Piscataway, NJ, 1998.
49. Bin-Jie, H., E. Y. Kai-Ning, Z. Jun, and T. Serge, "Scattering characteristics of conducting cylinder coated with nonuniform magnetized ferrite," *Chinese Physics*, Vol. 14, 2305–2313, 2005.